Engineering Applications

https://publish.mersin.edu.tr/index.php/enap

e-ISSN 2979-9201

Precise point positioning technique with single frequency raw GNSS observations using CNES and MADOCA real-time products on android smartphones

Barış Karadeniz [*1], **Hüseyin Pehlivan** [1], **Barışcan Arı** [1]

[1]*Gebze Technical University, Department of Geomatics Engineering, Türkiye, b.karadeniz@gtu.edu.tr; hpehlivan@gtu.edu.tr; b.ari2021@gtu.edu.tr*

Cite this study: Karadeniz, B., Pehlivan, H., & Arı, B. (2023). Precise point positioning technique with single frequency raw GNSS observations using CNES and MADOCA real-time products on android smartphones. Engineering Applications, 2 (3), 225-234

Keywords
Smartphone
Single-Frequency
GNSS
N-RT-PPP

Research Article
Received:08.03.2023
Revised: 19.07.2023
Accepted: 12.09.2023
Published:21.09.2023

Abstract

In this study, positioning performance was evaluated by making single-frequency GNSS (Global Navigation Satellite System) observations under real-time conditions with a smartphone. In experiments, GNSS observations were recorded with the Xiaomi Redmi Note 8 Pro via the Geo++ RINEX Logger application. Measurements were made with the geodetic-grade CHC I80 GNSS receiver to evaluate the performance of the smartphone. In addition to the collected raw observation data set, solutions were realized with the Near-Real-Time Precise Point Positioning (N-RT-PPP) technique by using satellite orbit and clock correction products produced under real-time conditions from the CNES (National Centre for Space Studies) and MADOCA (Multi-GNSS Advanced Demonstration tool for Orbit and Clock Analysis) archives. When all the observations with the epoch difference are examined, it is observed that the root mean square error (RMSE) values of the GPS/GLONASS observations give better results than the only-GPS solutions. In addition, in the epoch differenced time series produced from the smartphone, an improvement between 92% and 98% was observed for the part below 1 cm horizontally and 2 cm vertically after the convergence.

1. Introduction

Over the years, advancements in satellite constellations and modernized signals in global satellite systems have led to increased studies on positioning using geodetic-grade GNSS receiver/antenna(s), low-cost GNSS receiver/antenna(s), and even smartphones [1,2]. Initially, smartphones provided position information with a single-frequency, single-constellation of satellites and without open access to GNSS raw data. However, with the Android N version in 2016, Google announced the availability of raw GNSS data to users on Android-based smartphones [1,3], which has led to many studies on positioning using smartphones. So, smartphones, which are widely used by most people in the global community for their needs and have a large mass market in the mobile smart device market, have now become a subject that is researched in precise positioning studies for different applications in the GNSS market. Several studies have evaluated the quality of raw GNSS measurements collected by smartphones and their position accuracy performance. Banville and Diggelen [1] conducted experiments using a Samsung Galaxy S7 smartphone, and their results indicated that the main problems of smartphones for precise positioning are GNSS antenna quality and cycle slip. While pseudorange observations provide meter-level positioning accuracy, carrier-phase observations provide decimeter-level or better positioning accuracy. A similar study evaluated the quality of the raw measurements and the obtained position accuracy with the linear polarized antenna and external GNSS antenna in order to evaluate the antenna quality with the Huawei Mate 9 smartphone with the GNSS chip (Broadcom 4774) of the same model [4].

Other some studies have focus on evaluating the quality of GNSS observations collected from smartphones and analyzing their positioning performance. Zhang et al. [5] assess the quality of GNSS observations from an Android N smartphone and recommend using the C/N0 weighting model when testing position accuracy performance. Navarro-Gallardo et al. [6] evaluate the readiness of Galileo in Android devices using raw measurements.

Lachapelle et al. [7] compare the performance of a low-cost handheld unit with GNSS raw data capability with that of an Android smartphone in different environments. Gogoi et al. [8] conduct a controlled-environment quality assessment of Android GNSS raw measurements. Overall, these studies highlight the potential of smartphones for precise positioning but also acknowledge their limitations due to the GNSS antenna/chip feature used, which is sensitive to the multipath effect caused by signals reflected from objects in the environment.

Other studies reporting that poor data quality in smartphones is associated with signal-to-noise ratio are as follows. In this context, when the position accuracy performance of smartphones is tested, it is predicted that the C/N0 weighting model will be more appropriate than the elevation-dependent weighting model [9-12]. While positioning, navigation and timing applications with smartphones were made through single-frequency GNSS observations until 2018, Xiaomi produced and marketed Mi8 model smartphone that can collect dual-frequency GNSS raw observation data for the first time in May [13]. This event has been a start that will lead to the evaluation of precise positioning performance using different positioning techniques (Real-Time Kinematic, Precise Point Positioning, etc.) and many studies in engineering applications on smartphones [13-17]. In the literature, the positioning performance of smartphones has been evaluated by using geodetic-grade receivers as a reference to relative positioning or differential positioning technique, or by using a smartphone as a reference station [18-20]. Although the positioning studies with smartphones are low cost, due to the GNSS antenna/chip feature used, the signals reflected from the objects in the environment are sensitive to the multipath effect, which causes the collection of low quality GNSS measurements. GNSS receiver/antenna(s), which are high cost and designed to minimize the multipath effect, have advantages over the antenna/chip(s) used in smartphones. In addition, many positioning applications use carrier-phase observations for high positioning accuracy. However, due to the GNSS antenna/chip structure used in carrier phase observations on smartphones, it causes interruptions in phase observations [20,21].

Recent studies have shown that with the use of a single GNSS receiver, precise point positioning (PPP) technique can be used to determine positions under real-time conditions without the need for a simultaneous reference receiver, network or infrastructure. Along with the dual-frequency raw GNSS data collection of smartphones, PPP-based point positioning performance in both static and kinematic mode has been evaluated in many studies. In the studies, it was stated that the position accuracy can be determined at the decimeter level in static mode and with an accuracy of a few meters in kinematic mode [22-24]. In this study, single-frequency GNSS raw observations were collected using both smartphone and CHC I80 GNSS receiver/antenna, and evaluation was carried out with the N-RT-PPP method. In many scientific studies with smartphones, the relative positioning method has been taken as a comparison criterion to test positioning accuracy. Today, centimeter and even millimeter level positioning accuracy has been achieved by applying precise point positioning technique with a single GNSS receiver/antenna. However, in order to make a fair evaluation in the experiments, the solutions obtained from the measurements collected with the geodetic-grade GNSS receiver were chosen as the comparison criterion.

2. Material and Method

In this section, information and observation data sets of GNSS receiver/antenna used in the experiments are introduced. In addition, the observations collected on GNSS receiver/antenna(s) are demonstrated by the N-RT-PPP method. Within the scope of this study, observations were made with a total of 2 GNSS receiver/antenna(s) at a sampling range of 1 Hz using CHC I80 GNSS receivers and Xiaomi Redmi Note 8 Pro model smartphone. Experiments were carried out in Gebze Technical University campus in the Department of Geomatics Engineering in November 2022 and lasted for about 1.5 hours. The experimental setup is shown in Figure 1. During the experiment, GPS and GLONASS satellite observations were collected with 2 GNSS receiver/antenna(s). With the IGS (International GNSS Service)-RTS (Real-Time Service) service project initiated by IGS, RTS products can be broadcast over the internet in RTCM/SSR (Radio Technical Commission for Maritime Services/ State Space Representation) data format with NTRIP (Networked Transport of RTCM via Internet Protocol) data transmission protocol, and real- time satellite orbit and clock correction information can be obtained [25]. Satellite orbit and clock correction products for GPS and GLONASS are provided by CNES and MADOCA, similar to IGS-RTS. The zero-difference ambiguity resolution technique is applied in CNES solutions to improve the quality of clocks for IGS-RTS. These products allow for ambiguity resolution at the user receiver, achieving 1 cm horizontal precision point positioning accuracy. Satellite orbits and clocks are available in real-time in the CNES archive as sp3, clk, and bia files a few minutes after midnight according to UTC (Coordinated Universal Time). These products are useful for post-processing PPP software, but for users who want to test in real-time conditions, there are errors in the bia extension files to be added to the observations that provide direct ambiguity resolution in both the code and carrier phase GNSS observations. The bia files are available in the CNES archive for ambiguity resolution in PPP-AR software. On the other hand, JAXA (Japan Aerospace Exploration Agency) has developed a precise GNSS orbit and clock prediction system called MADOCA, which supports GPS, GLONASS, and QZSS satellite systems. JAXA provides two different types of products, "Real Time MADOCA product" with small delay and "Offline MADOCA

product" with higher precision. Satellite orbit and clock correction products produced with MADOCA software are available in RTCM SSR format for free to users in real-time.

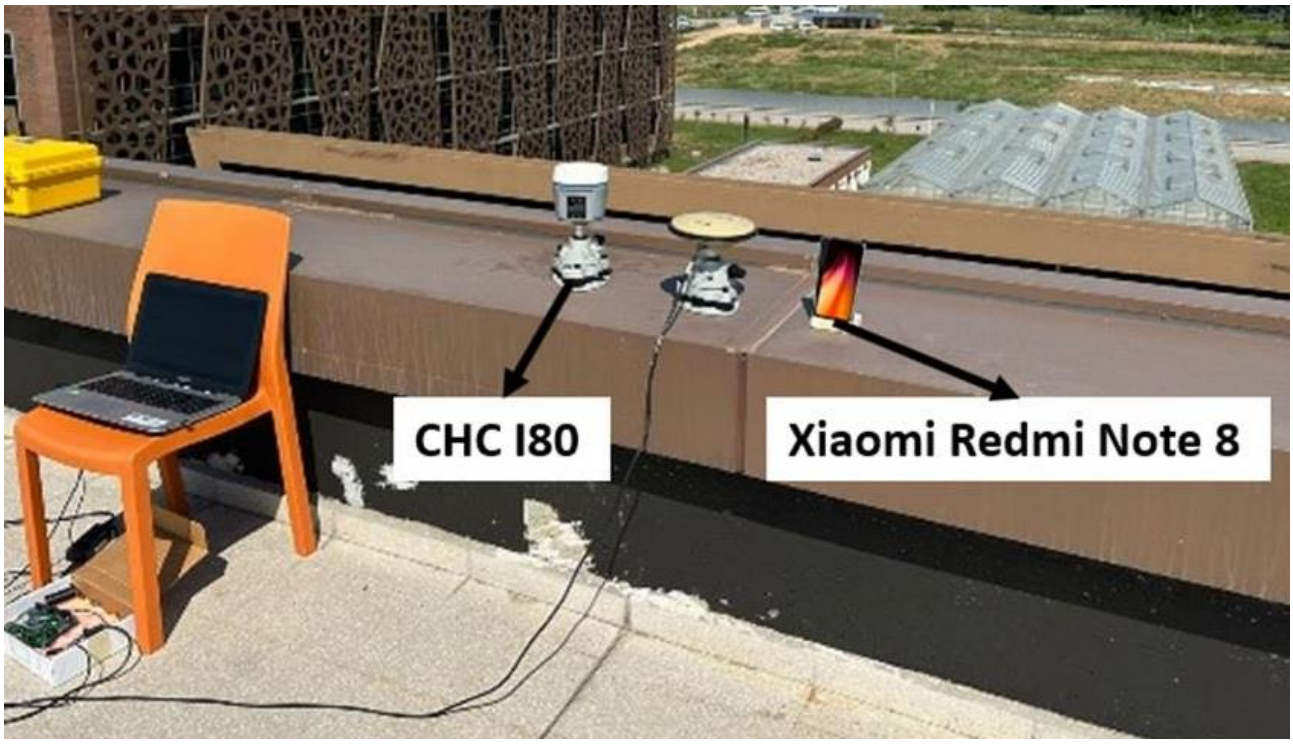

Figure 1. The experimental setup.

Table 1. Process options made in the N-RT-PPP method.

Entry parameters	Interval (s)	0.05
	Positioning Mode	PPP-Static
	Frequencies	L1
	Filter Type	Forward
	Elevation Mask (°)/SNR Mask (dBHz)	10°/OFF
	Receiver Dynamics/Earth Tides Correction	OFF/Solid+OTL
	Ionosphere/Troposphere Correction	Broadcast/ Saastamoinen
	Satellite Ephemeris/Clock	Broadcast/Broadcast+SSR APC*
	Satellite Antenna Phase Center Variation (PCV)	✓
	Receiver Antenna Phase Center Variation	✓
	Phase Windup	✓
	Reject Eclipse (for GPS Block IIA)	✓
	Receiver Autonomous Integrity Monitoring (RAIM)/ Fault Detection and Exclusion (FDE)	✓
	DCB (Differential Code Bias) Correction	✓
	GNSS Type	GPS/GLONASS
Files	Satellite Antenna PCV File	igs14.atx
	Receiver Antenna PCV File	igs14.atx
	DCB (Differential Code Bias) Data File	P1C12102.DCB
	EOP (Earth Orientation Parameters) Data File	EOP.txt

Note: The * symbol in Table 1 refers to the parameters of the N-RT-PPP solution using only MADOCA products.

In this study, satellite orbit and clock correction information produced in real-time conditions from the CNES and MADOCA archives was used to realize an N-RT-PPP solution. The process steps of this technique in the experiments are shown in detail in Figure 2. A solution was made with the rtkpost application module of the RTKLIB software to the point positioning and to monitor it in real time using the N-RT-PPP method. Used in solutions; Input data, additional parameters, threshold values, measurement errors, measurement noises and options for additional data inputs are given in Table 1. Raw observation data collected under the same conditions with both a smartphone and a geodetic-grade GNSS receiver were processed with the PPP-based method using the same products. However, it was observed that there was data loss in some epochs in the solutions made with a smartphone after the process due to the GNSS chip feature in the smartphone. This is due to the GNSS chip feature

in the smartphone. Therefore, it was tried to eliminate the data losses by applying the interpolation method. The solutions obtained after the experiment were evaluated by making statistical calculations in MATLAB programming language. The evaluation of positioning accuracy from the solutions obtained in this study was carried out in two stages. First, the observation data of the simultaneous CHC I80 receiver/antenna and Xiaomi Redmi Note 8 smartphone during the experiment were evaluated by taking the epoch differences without taking the threshold value. Secondly, the positioning accuracy was evaluated for three components by taking the threshold value due to the convergence time due to the nature of the PPP-based solution, the low data quality of the smartphones and the locking time to the satellites. Details of the assessment are described in the next section.

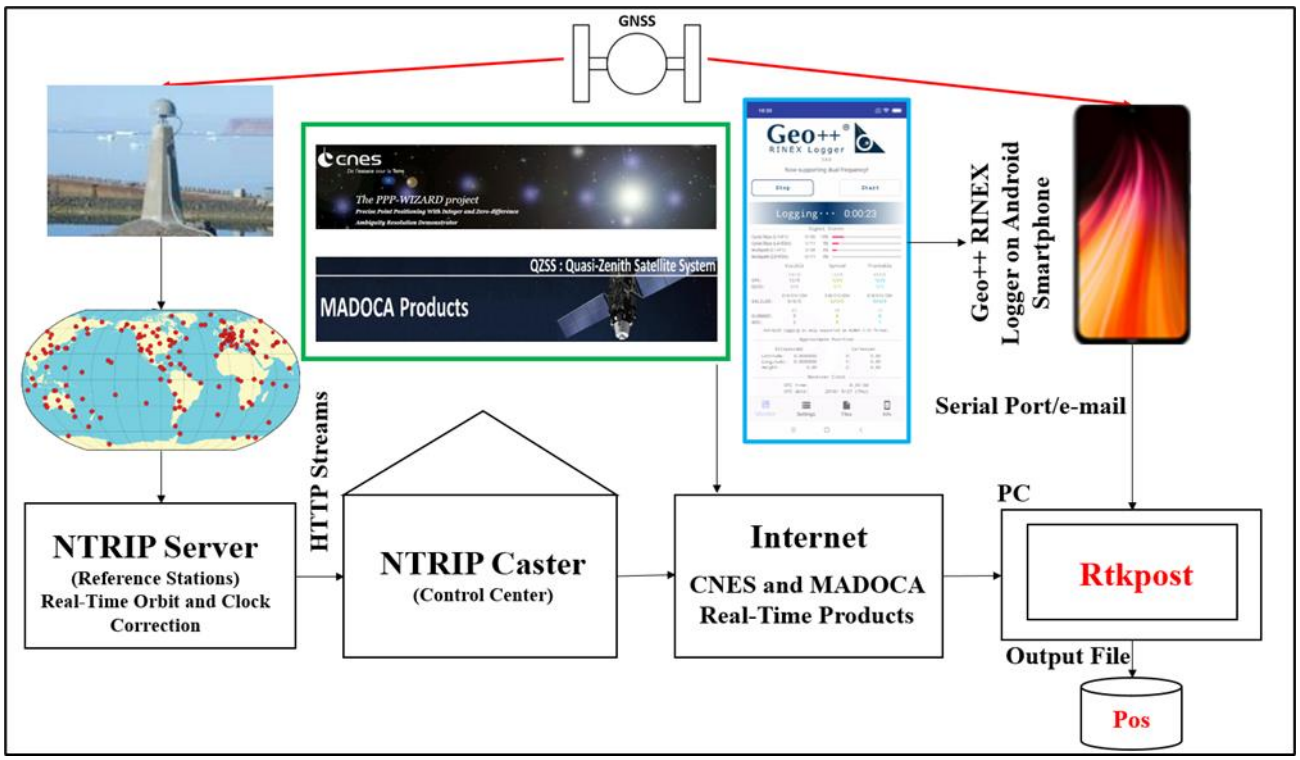

Figure 2. Schematic view of the N-RT-PPP method.

This study includes the N-RT-PPP technique based on multi-GNSS code and phase observations. In this context, the equations can be written as:

$$P_r^s = \rho_r^s + c.\delta t_r - c.\delta t^s + T_r^s + I_r^s + m_r^s + \varepsilon_{r,P}^s \quad (1)$$

$$\Phi_{r,j}^s = \rho_r^s + c.\delta t_r - c.\delta t^s + \lambda N_r^s + T_r^s - I_r^s + m_r^s + \varepsilon_{r,\Phi}^s \quad (2)$$

In Equation 1 and 2, the subscript r represents the receiver, while the superscript s represents the satellite; The pseudorange and carrier-phase measurements of the receiver relative to the satellite in P and Φ length units, respectively; ρ is the geometric distance between the receiver and the satellite; c is the speed of light in vacuum, δt_r and δt^s are receiver and satellite clock corrections, respectively; T_r^s indicates tropospheric delay along the path between receiver and satellite; I_r^s is the ionospheric delay along the path from the satellite to the receiver; λ is the carrier-phase wavelength; N_r^s is the initial phase ambiguity; m_r^s and ε_r^s represent the multipath and noise of the code and phase observations, respectively. RTS products offered by IGS RTS to the user include satellite orbit and clock corrections by providing continuous broadcast ephemeris stream. Obtaining precise real-time satellite orbit and clock information is critical for the accuracy of the RT-PPP method. The orbit correction message in SSR format includes orbit corrections in the radial (δ_r), along-track (δ_a), and cross-track (δ_c) directions and velocities $\delta_{\dot{r}}$, $\delta_{\dot{a}}$, $\delta_{\dot{c}}$ in the epoch t_0 [26]. The orbit corrections in the RTCM-SSR are calculated from the message in the t_0 reference epoch to the current epoch t as follows.

$$\delta \boldsymbol{O} = \begin{bmatrix} \delta_r \\ \delta_a \\ \delta_c \end{bmatrix} + \begin{bmatrix} \delta_{\dot{r}} \\ \delta_{\dot{a}} \\ \delta_{\dot{c}} \end{bmatrix} (t - t_0) \quad (3)$$

Since the orbit corrections calculated in Equation 3 are in the orbit coordinate system, the radial (e_r), along-track (e_a) and cross-track (e_c) unit vectors are calculated in the e direction for conversion to geocentric geostationary coordinate system [26].

$$e_a = \frac{\dot{r}}{|\dot{r}|}, \qquad e_c = \frac{r\ x\ \dot{r}}{|r\ x\ \dot{r}|}, \qquad e_r = e_a\ x\ e_c \tag{4}$$

In Equation 4, r represents the satellite broadcast position vector, while $\dot{r}$ represents the satellite broadcast velocity vector. The conversion of corrections to geocentric correction is as shown in Equation 5.

$$\delta X = [e_R \quad e_A \quad e_c]\delta \boldsymbol{O} \tag{5}$$

After the transformation, the corrected precise orbital position is obtained by adding the corrections obtained from the transformation to the orbital component of the broadcast.

$$X^s_{prec}(t) = X^s_{brdc}(t) + \delta X \tag{6}$$

In Equation 6, $X^s_{prec}(t)$ and $X^s_{brdc}(t)$ represent precise and broadcast satellite position, respectively. For the current epoch t, clock correction, the SSR clock correction message is broadcast as three polynomial coefficients a_0, a_1, a_2 and its mathematical model is as follows.

$$\delta C = a_0 + a_1(t - t_0) + a_2(t - t_0)^2 \tag{7}$$

The corrected precision clock offset at time t is calculated as in the equation below by adding the clock offset calculated by the broadcast ephemerides in the same epoch to the clock correction at time t calculated in Equation 7.

$$\delta dT^s{}_{prec}(t) = dT^s{}_{brdc}(t) + \frac{\delta C}{c} \tag{8}$$

In Equation 8, $\delta dT^s{}_{prec}(t)$ represents the corrected precision clock offset, $dT^s{}_{brdc}(t)$ represents the arc clock offset, and c stands for the speed of light.

3. Results

In this section, the study evaluates the performance of single-frequency GPS and GPS/GLONASS solutions using raw GPS/GLONASS observations obtained from the Xiaomi Redmi Note 8 smartphone, processed with the N-RT-PPP technique in static mode, along with satellite orbit and clock information produced under real-time conditions. To fairly assess the positioning performance of smartphones with single-frequency GNSS observations, a N-RT-PPP solution was made in static mode using a single GNSS receiver (CHC I80). Figure 3 shows the epoch differenced time series of the solutions generated from both the geodetic-grade GNSS receiver and the smartphone throughout the entire experiment. In addition, statistical histograms of the epoch differences obtained from the smartphone are provided, using the solutions obtained with the geodetic-grade GNSS receiver as reference. The first row of the figure shows the epoch differenced time series of the north, east, and up components, respectively, based on only-GPS observations.

The second row of the figure shows the RMSE values and histogram distributions of the three different components of the epoch differenced produced from the Xiaomi 8 smartphone with reference to the epoch differences obtained from the CHC I80 GNSS receiver. In contrast, the third row presents the time series of the epoch differences obtained using GPS/GLONASS observations, along with the statistical values of the observations obtained from the smartphone in the fourth row. According to the results, there were clearly fluctuations in the solutions obtained from the smartphone. These fluctuations are due to the low data quality of the MediaTek Helio G90T chipset in the Xiaomi Redmi Note 8 Pro smartphone, that is, the signal-to-noise ratio (SNR) is lower than the geodetic-grade CHC I80 receiver. Fluctuations due to PPP-based solution are expected in the epoch differences obtained from both measurement data. However, in the static solution, in addition to the fluctuation in the solutions made with a smartphone, some epochs have jumped. In addition, there are epoch losses in the measurements collected with a smartphone. This is due to the inability of the chipset in the smartphone to collect measurements in that epoch.

This situation was resolved by the interpolation method before data evaluation. Despite being a static solution, these fluctuations persisted between approximately 800 (s) and 1000 (s) epochs, although different for the three components. Therefore, from the instant that the fluctuations fall below 1 cm in the horizontal component and below 2 cm in the vertical component, the epoch differenced time series and statistical histograms are shown as seen in Figure 4. According to the results, it was observed that the RMSE values of GPS and GPS/GLONASS solutions, whose epoch differenced were taken after fluctuation, were improved according to the results throughout the whole experiment. On the other hand, N-RT-PPP solution using real-time MADOCA products is

given in Figure 5. In the first line of the figure, the epoch difference time series of the only-GPS solutions of the whole experiment are given. As seen in the time series, long-term fluctuations in the solutions made with a smartphone are clearly seen in all three components. Although the same situation is observed in GPS/GLONASS observations, it has been observed that RMSE values in both GPS and GPS/GLONASS solutions give similar results. Looking at the north and up components, only-GPS, and looking at the east component, even the results made with GPS/GLONASS observations were found to be good.

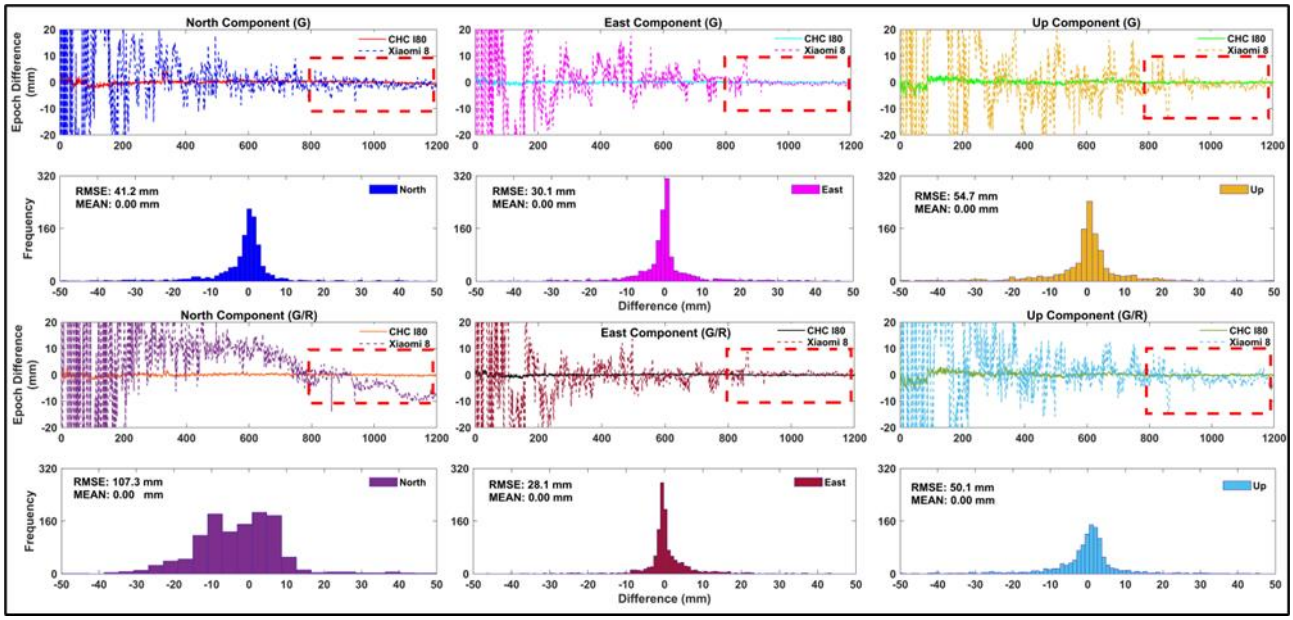

Figure 3. The epoch differenced time series and histogram distributions throughout the experiment.

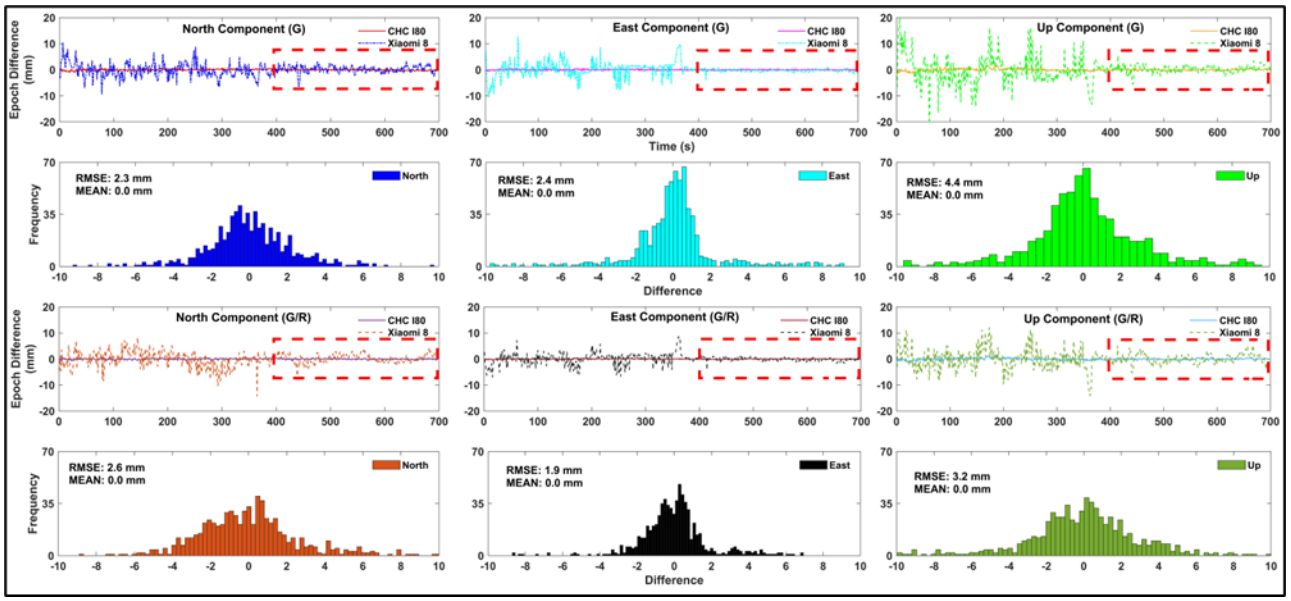

Figure 4. The epoch differenced time series and histogram distributions after convergence.

In addition, measurements after approximately 800 to 1000 epochs, where the fluctuations decreased and the integer phase ambiguity began to converge, were evaluated in the solutions made with the smartphone. In this context, the epoch difference time series of the solutions obtained from both only -GPS and GPS/GLONASS observations are shown in Figure 6 in three components. Looking at the time series, it was observed that the solutions obtained with the geodetic-grade GNSS receiver, and the solutions obtained from the smart phones were consistent with each other, but there were fluctuations and occasional jumps at first in the solutions produced with the smart phone. It is clear that this jump is more in the North and up component. Moreover, when the RMSE values of the epoch difference results obtained from the smartphone were examined, it was observed that the values obtained after the convergence were at the millimeter level in both only-GPS and GPS/GLONASS observations.

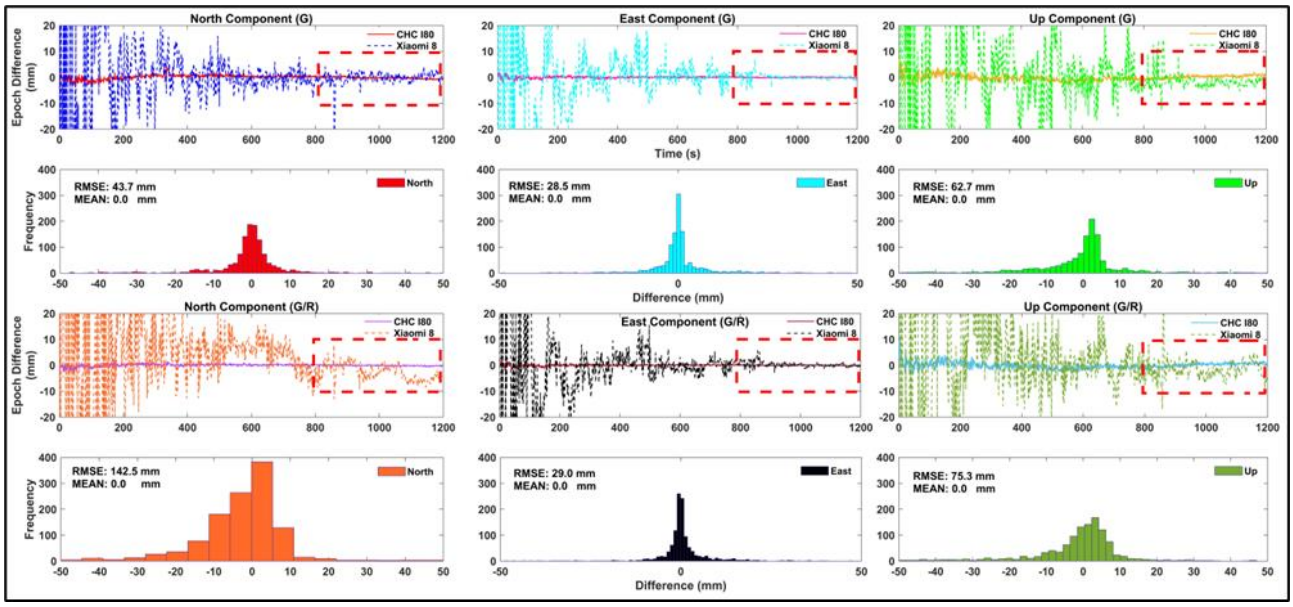

Figure 5. The epoch differenced time series and histogram distributions throughout the experiment.

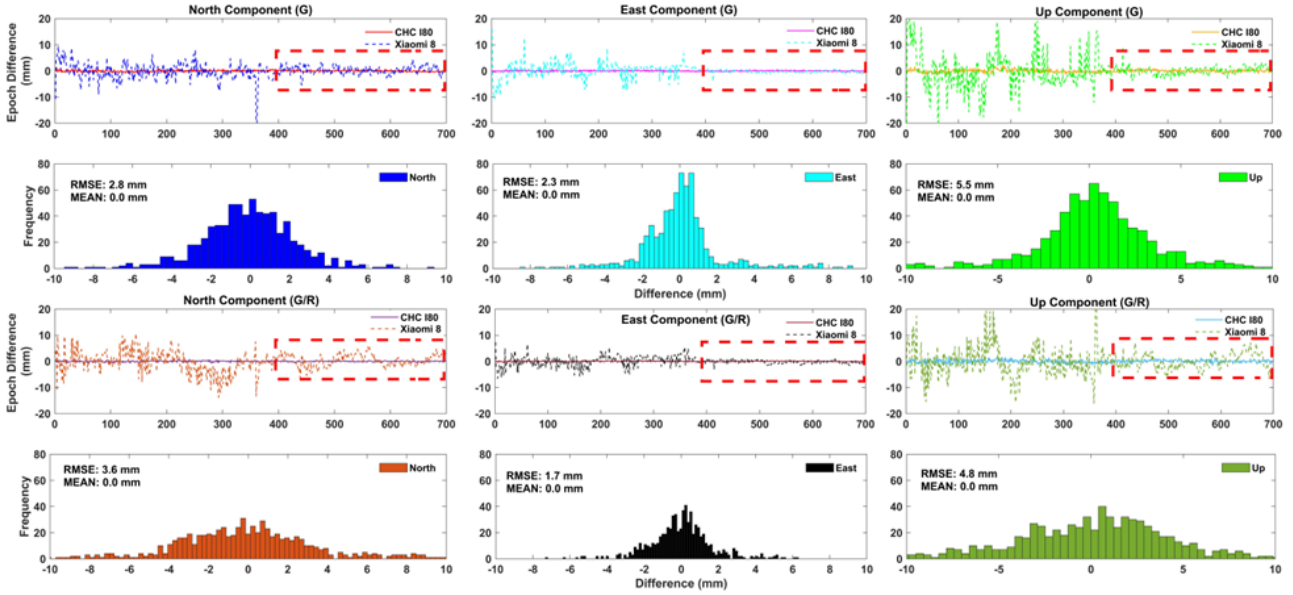

Figure 6. The epoch differenced time series and histogram distributions after convergence.

In Table 2, the RMSE values of N-RT PPP solutions obtained from both CNES and MADOCA real-time products are given for the epoch differences of GPS and GPS/GLONASS solutions during the whole experiment and after fluctuations. Here, A is the RMSE values obtained using CNES real-time products and all test observation data, B is the RMSE values obtained using CNES real-time products and post-fluctuation observation data, C is the RMSE values obtained using MADOCA real-time products and all experiment observation data, and D represents RMSE values obtained using MADOCA real-time products and post-convergence observation data. According to the results, it has been revealed that the solutions made after convergence time using both real-time products are consistent with each other at the millimeter level. In addition, it was observed that RMSE values were improved by adding GLONASS satellite observations to GPS observations after the convergence time.

Table 2. RMSE values of North, East and Up components for Xiaomi 8 smartphone.

	GPS			**GPS/GLONASS**		
	North (mm)	East (mm)	Up (mm)	North (mm)	East (mm)	Up (mm)
A	41.2	30.1	54.7	107.3	28.1	50.1
B	2.3	2.4	4.4	2.6	1.9	3.2
C	43.7	28.5	62.7	142.5	29.0	75.3
D	2.8	2.3	5.5	3.6	1.7	4.8

4. Discussion

Many studies have been carried out in the literature to improve positioning performance with Android smartphones. In this paper, the discussion focuses on the results of the study, which aimed to evaluate the positioning performance of Android smartphones using the N-RT-PPP technique with GPS and GPS/GLONASS observations. Two different orbit and clock correction information produced under real-time conditions were used for the study, and a geodetic GNSS receiver was used to ensure a fair comparison. However, it should be noted that there is a significant difference between the chipset in the smartphone and the geodetic GNSS receiver/antenna, which is reflected in the epoch difference time series. Additionally, due to the duty cycle problem of the smartphone, not all epochs could be used in the time series, resulting in a long convergence time. This issue has been resolved in Android 9 and higher versions. The geodetic GNSS receiver/antenna has a higher signal-to-noise ratio and a better satellite locking capability, leading to less branching in the time series. Therefore, the positioning performance of the smartphone used in the application may decrease depending on various parameters. In future studies, adding different satellite systems and collecting dual-frequency observations may improve the positioning performance.

5. Conclusion

This study aimed to evaluate the near-real-time positioning performance of GNSS observations collected statically with a smartphone. The data set collected with the Xiaomi Redmi Note 8 smartphone was solved with a single-frequency combination of both GPS and GPS/GLONASS satellites, while observations were also made with a single geodetic-grade GNSS receiver to evaluate the results fairly. The results indicated that the addition of GLONASS satellite to single-frequency GPS satellite observations collected in static mode with smartphones improved real-time positioning performance. It was observed that the results obtained with the combination of GPS/GLONASS satellites give better results than the only-GPS observations. After fluctuation, significant improvements were shown in the north, east and up components, respectively, in the solutions realized by only-GPS observations (94.4%, 92.0%, and 92.0%), and in the GPS/GLONASS satellite combination (97.6%, 93.2%, and 93.6%), respectively. Furthermore, the smartphone's static positioning accuracy improved significantly under real-time conditions after approximately 600 (s) to 800 (s) epochs. Future studies will consider evaluating the positioning performance of smartphones capable of dual-frequency multi-GNSS observations with current technological developments in different satellite combinations in real-time.

Acknowledgement

This study was partly presented at the 6th Advanced Engineering Days [27].

Funding

This research received no external funding.

Author contributions

Barış Karadeniz: Conceptualization, Methodology, Software **Hüseyin Pehlivan:** Data curation, Writing-Original draft preparation, Validation. **Barışcan Arı:** Visualization, Investigation, Software.

Conflicts of interest

The authors declare no conflicts of interest.

References

1. Banville, S., & van Diggelen, F. (2016). Precision GNSS for everyone: Precise positioning using raw GPS measurements from Android smartphones. GPS World, 27(11), 43-48.
2. GNSS Agency, (2017). Using GNSS raw measurements on Android devices. European GNSS Agency GNSS Raw Measurements Task Force. http://doi.org/10.2878/449581
3. Gül, C., Doğan, A. H., & Öcalan, T. (2021). Investigation of PPP performance with dual frequency raw GNSS observations obtained from smartphones. Journal of Geodesy and Geoinformation, 8(2), 120-130.

4. Siddakatte, R., Broumandan, A., & Lachapelle, G. (2017, November 27-30). Performance evaluation of smartphone GNSS measurements with different antenna configurations. Proceedings of the International Navigation Conference, Brighton
5. Navarro-Gallardo, M., Bernhardt, N., Kirchner, M., Musial, J. R., & Sunkevic, M. (2017, September). Assessing Galileo readiness in Android devices using raw measurements. In Proceedings of the 30th International Technical Meeting of the Satellite Division of The Institute of Navigation (ION GNSS+ 2017, 85-100. https://doi.org/10.33012/2017.15183
6. Lachapelle, G., Gratton, P., Horrelt, J., Lemieux, E., & Broumandan, A. (2018). Evaluation of a low cost hand held unit with GNSS raw data capability and comparison with an android smartphone. Sensors, 18(12), 4185. https://doi.org/10.3390/s18124185
7. Gogoi, N., Minetto, A., Linty, N., & Dovis, F. (2018). A controlled-environment quality assessment of android GNSS raw measurements. Electronics, 8(1), 5. https://doi.org/10.3390/electronics8010005
8. Zhang, X., Tao, X., Zhu, F., Shi, X., & Wang, F. (2018). Quality assessment of GNSS observations from an Android N smartphone and positioning performance analysis using time-differenced filtering approach. Gps Solutions, 22, 70. https://doi.org/10.1007/s10291-018-0736-8
9. Banville, S., Lachapelle, G., Ghoddousi-Fard, R., & Gratton, P. (2019, September). Automated processing of low-cost GNSS receiver data. In Proceedings of the 32nd International Technical Meeting of the Satellite Division of The Institute of Navigation (ION GNSS+ 2019, 3636-3652. https://doi.org/10.33012/2019.16972
10. Li, G., & Geng, J. (2019). Characteristics of raw multi-GNSS measurement error from Google Android smart devices. GPS Solutions, 23, 90. https://doi.org/10.1007/s10291-019-0885-4
11. Paziewski, J., Sieradzki, R., & Baryla, R. (2019). Signal characterization and assessment of code GNSS positioning with low-power consumption smartphones. GPS solutions, 23, 98. https://doi.org/10.1007/s10291-019-0892-5
12. Robustelli, U., Paziewski, J., & Pugliano, G. (2021). Observation quality assessment and performance of GNSS standalone positioning with code pseudoranges of dual-frequency Android smartphones. Sensors, 21(6), 2125. https://doi.org/10.3390/s21062125
13. Chen, B., Gao, C., Liu, Y., & Sun, P. (2019). Real-time precise point positioning with a Xiaomi MI 8 android smartphone. Sensors, 19(12), 2835. https://doi.org/10.3390/s19122835
14. Liu, Q., Gao, C., Peng, Z., Zhang, R., & Shang, R. (2021). Smartphone positioning and accuracy analysis based on real-time regional ionospheric correction model. Sensors, 21(11), 3879. https://doi.org/10.3390/s21113879
15. Odolinski, R., & Teunissen, P. J. (2019). An assessment of smartphone and low-cost multi-GNSS single-frequency RTK positioning for low, medium and high ionospheric disturbance periods. Journal of Geodesy, 93(5), 701-722. https://doi.org/10.1007/s00190-018-1192-5
16. Robustelli, U., Baiocchi, V., & Pugliano, G. (2019). Assessment of dual frequency GNSS observations from a Xiaomi Mi 8 Android smartphone and positioning performance analysis. Electronics, 8(1), 91. https://doi.org/10.3390/electronics8010091
17. Wu, Q., Sun, M., Zhou, C., & Zhang, P. (2019). Precise point positioning using dual-frequency GNSS observations on smartphone. Sensors, 19(9), 2189. https://doi.org/10.3390/s19092189
18. Gao, R., Xu, L., Zhang, B., & Liu, T. (2021). Raw GNSS observations from Android smartphones: Characteristics and short-baseline RTK positioning performance. Measurement Science and Technology, 32(8), 084012. https://doi.org/10.1088/1361-6501/abe56e
19. Geng, J., & Li, G. (2019). On the feasibility of resolving Android GNSS carrier-phase ambiguities. Journal of Geodesy, 93(12), 2621-2635. https://doi.org/10.1007/s00190-019-01323-0
20. Paziewski, J., Fortunato, M., Mazzoni, A., & Odolinski, R. (2021). An analysis of multi-GNSS observations tracked by recent Android smartphones and smartphone-only relative positioning results. Measurement, 175, 109162. https://doi.org/10.1016/j.measurement.2021.109162
21. Zangenehnejad, F., & Gao, Y. (2021). GNSS smartphones positioning: Advances, challenges, opportunities, and future perspectives. Satellite navigation, 2, 1-23. https://doi.org/10.1186/s43020-021-00054-y
22. Aggrey, J., Bisnath, S., Naciri, N., Shinghal, G., & Yang, S. (2019, September). Use of PPP processing for next-generation smartphone GNSS chips: key benefits and challenges. In Proceedings of the 32nd International Technical Meeting of the Satellite Division of The Institute of Navigation (ION GNSS+ 2019, 3862-3878.
23. Elmezayen, A., & El-Rabbany, A. (2019). Precise point positioning using world's first dual-frequency GPS/GALILEO smartphone. Sensors, 19(11), 2593. https://doi.org/10.3390/s19112593
24. Kulikov, R., Chugunov, A., & Zamolodchikov, V. (2019, November). Investigation of collision warning possibilities by means of GNSS receivers of Android smartphones. In IOP Conference Series: Materials Science and Engineering, 695(1), 012013. https://doi.org/10.1088/1757-899X/695/1/012013
25. Elsobeiey, M., & Al-Harbi, S. (2016). Performance of real-time Precise Point Positioning using IGS real-time service. GPS solutions, 20, 565-571. https://doi.org/10.1007/s10291-015-0467-z
26. Hadas, T., & Bosy, J. (2015). IGS RTS precise orbits and clocks verification and quality degradation over time. GPS solutions, 19, 93-105. https://doi.org/10.1007/s10291-014-0369-5

27. Karadeniz, B., Pehlivan, H., & Arı, B. (2023). Precise point positioning technique with single frequency raw GNSS observations using different products on android smartphones. Advanced Engineering Days (AED), 6, 61-63.